



Nano ZnO-activated carbon composite electrodes for supercapacitors

M. Selvakumar^b, D. Krishna Bhat^{a,*}, A. Manish Aggarwal^a, S. Prahladh Iyer^a, G. Sravani^a

^a Department of Chemistry, National Institute of Technology Karnataka, Surathkal, Srinivasnagar 575 025, India

^b Department of Chemistry, Manipal Institute of Technology, Manipal University, Manipal 576 104, India

ARTICLE INFO

Article history:

Received 16 November 2009

Received in revised form

16 January 2010

Accepted 9 February 2010

Keywords:

ZnO

Nanomaterials

Activated carbon

Supercapacitor

Specific capacitance

ABSTRACT

A symmetrical (p/p) supercapacitor has been fabricated by making use of nanostructured zinc oxide (ZnO)-activated carbon (AC) composite electrodes for the first time. The composites have been characterized by field emission scanning electron microscopy (FESEM) and X-ray diffraction analysis (XRD). Electrochemical properties of the prepared nanocomposite electrodes and the supercapacitor have been studied using cyclic voltammetry (CV) and AC impedance spectroscopy in 0.1 M Na₂SO₄ as electrolyte. The ZnO-AC nanocomposite electrode showed a specific capacitance of 160 F/g for 1:1 composition. The specific capacitance of the electrodes decreased with increase in zinc oxide content. Galvanostatic charge-discharge measurements have been done at various current densities, namely 2, 4, 6 and 7 mA/cm². It has been found that the cells have excellent electrochemical reversibility and capacitive characteristics in 0.1 M Na₂SO₄ electrolyte. It has also been observed that the specific capacitance is constant up to 500 cycles at all current densities.

© 2010 Elsevier B.V. All rights reserved.

1. Introduction

Supercapacitors or electrochemical capacitors are energy storage devices that have gained importance in recent years owing to their technological significance ranging from satellites to consumer electronic devices [1]. In general, two kinds of electrode materials are used for the fabrication of supercapacitors: (i) carbon materials with high surface area, such as activated carbon, carbon aerogel, etc.; (ii) metal oxides such as oxides of Ru, Ni, Co, Zn etc., and conducting polymers [2]. Ruthenium oxides are widely used in electrochemical supercapacitor due to its high specific capacitance and prominent electrochemical properties [3]. However, the high cost of Ru has retarded its commercial acceptance and a cheap metal oxide with various oxidation states are promising materials for supercapacitor applications. Nickel oxide [4,5], cobalt oxide [6] and manganese oxide supercapacitors [7], are inexpensive and exhibit pseudo capacitive behavior similar to that of ruthenium oxide. Though the physical properties of the zinc oxide (ZnO) nanoparticles are available in literature [8–11], available information on the suitability of the ZnO as a potential candidate for supercapacitor application is very little [12]. ZnO is a well-known battery active material having high energy density of 650 A/g, but it has the disadvantage of formation of dendrite growth during consecutive cycling, which leads to decrease in cycle life. However, because of its good

electrochemical activity and eco-friendly nature, zinc oxide can be a promising electrode material for supercapacitor.

In this work, nanostructured ZnO has been prepared by a microwave assisted synthesis method [13] and ZnO-activated carbon(AC) composite electrodes have been prepared as a candidate electrodes for the fabrication of supercapacitor. The supercapacitor properties have been evaluated by cyclic voltammetry, electrochemical impedance spectroscopy and charge-discharge cycling tests.

2. Experimental procedures

A typical experimental strategy was as follows: zinc acetate and hydrazine hydrate were mixed at a molar ratio of 1:4 in water under stirring. Hydrazine readily reacted with zinc acetate to form a slurry like precipitate of the hybrid complex between them. The stirring of the slurry was continued for 15 min and then the mixture was subjected to microwave irradiation at 75 W microwave power for 10 min. The slurry became clear with a white precipitate at the bottom. The precipitate was filtered off, washed with absolute ethanol and distilled water several times and then dried in a vacuum at 60 °C for 4 h.

X-ray diffraction patterns of ZnO nanoparticles were taken on a Japan Rigaku D/max rA X-ray Diffractometer equipped with graphite monochromatized high intensity Cu K α radiation ($\lambda=1.54178$ Å). The accelerating voltage was set at 0.06°/s in the 2θ range 10–80°. The field emission scanning electron microscopy (FE-SEM) images were taken on a FEI Company FE-SEM.

* Corresponding author. Tel.: +91 824 2474000x3202; fax: +91 824 2474033.
E-mail address: denthajekb@gmail.com (D. Krishna Bhat).

2.1. Preparation of electrode

AC (Aldrich) was mixed with ZnO in three different ratio (1:1–1:3) by using n-methylpyrrolidone along with a binder, polyvinylidene fluoride (PVDF), in the ratio of 70:30 using a pestle and mortar. This paste was then applied with a brush to pre-weighed stainless steel current collector and dried at room temperature.

2.2. Electrochemical characterization of electrode

Electrochemical half cell measurements were conducted in a three-electrode cell equipped with a reference electrode (SCE), platinum foil as counter electrode and AC–ZnO composite as the working electrode. Electrochemical characterizations of the electrode were carried out by cyclic voltammetry (CV), electrochemical impedance spectroscopy (EIS) and galvanostatic charge–discharge studies. All the electrochemical studies were carried out using an Autolab electrochemical system (ECO Chemie BV, The Netherlands). AC impedance measurements were made in the frequency range of 0.01– 10^6 Hz characterization.

3. Results and discussion

3.1. Structural analysis

The crystal structure of the prepared ZnO was characterized by X-ray diffraction analysis. Fig. 1 shows the XRD pattern of as prepared ZnO. All the peaks of the ZnO nanoparticles can be indexed to the wurtzite single phase ZnO (JCPDS Card No. 36-1451, $a=3.249$ Å, $c=5.206$ Å, space group: P63mc, No.186). No characteristic peaks of other impurities such as $Zn(OH)_2$ were detected in the diffractogram. The average diameter of the particles calculated using Scherrer formula based on the maximum intensity peak in the XRD pattern is around 25 nm. However, the FESEM (Fig. 2) image of the ZnO samples indicates a wide distribution of particle sizes ranging from 10 to 200 nm and exhibited only irregular granular feature. Fig. 3 shows the SEM image of nano ZnO-activated carbon composite pasted on to the SS panel. The image clearly shows the coating of the nanostructured ZnO on to activated carbon. This kind of surface morphology is quite ideal for the fabrication of the electrode as it would be having high surface area and expected to yield good capacitance.

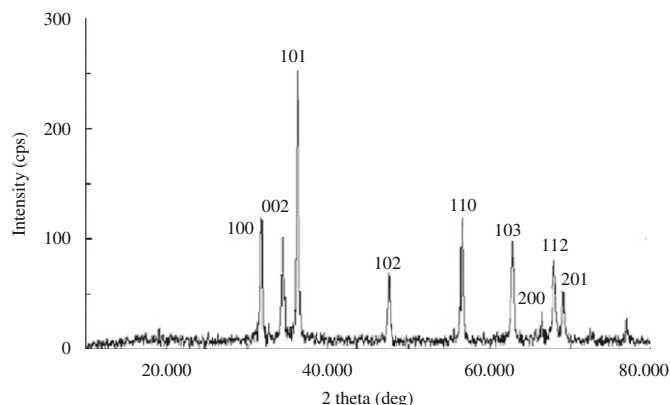


Fig. 1. XRD pattern of ZnO.

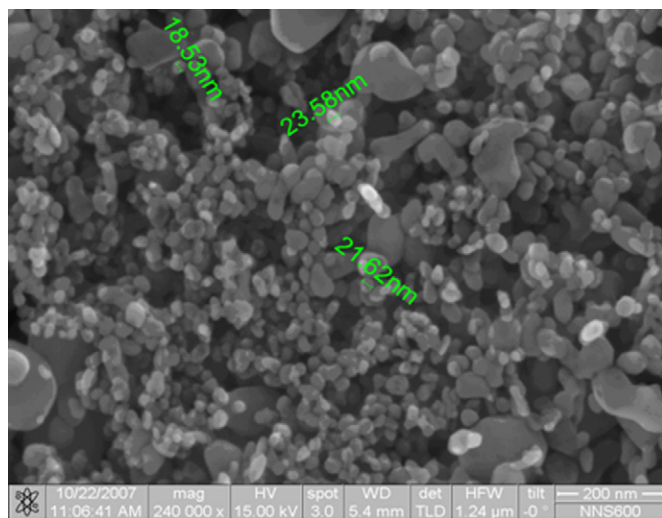


Fig. 2. FESEM image of ZnO.

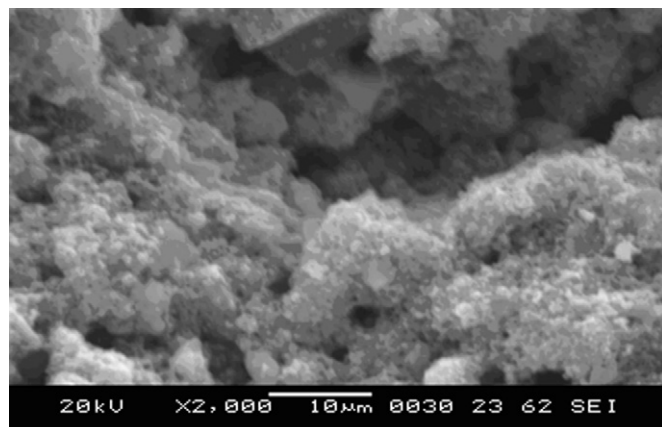


Fig. 3. SEM image of ZnO-activated carbon composite.

3.2. Electrochemical properties of ZnO–AC composites and supercapacitor

Fig. 4 shows the cyclic voltammogram (CV) response of ZnO nanomaterials prepared under different microwave powers. The CVs have been measured in 0.1 M Na_2SO_4 at a scan rate of 50 mV s^{-1} . The CV corresponding to ZnO material prepared under 10% microwave power indicated better response than at other power settings. Hence, ZnO synthesis was done under 10%(75 W) microwave power. The synthesis at higher microwave power may cause changes in the surface features of the product resulting in poor cyclic voltammetric response. Fig. 5 shows CV responses of nano ZnO-activated carbon composite electrodes with different ratios such as 1:1, 2:1 and 3:1. prepared on stainless steel panels. The specific capacitance calculations show that the composite electrode with 1:1 (ZnO:AC) composition has higher specific capacitance. AC Impedance spectroscopy also supports this observation. Fig. 6 shows the Nyquist plot for electrodes with three different compositions. The one with 1:1 composition exhibits lowest resistance and high capacitance. Fig. 7 shows the CV of the p/p symmetrical supercapacitor fabricated with ZnO–AC composite electrodes. The observed rectangular type plots are indicative of good capacitive behavior. This is in fact a synchronization of double layer and redox type supercapacitor features.

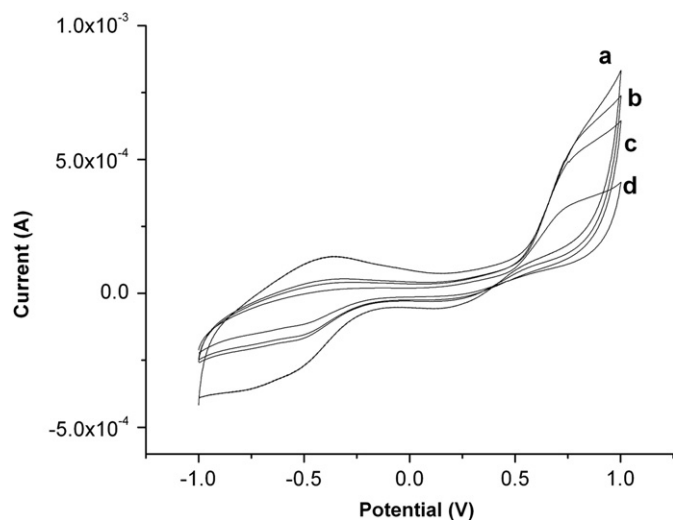


Fig. 4. CV of ZnO prepared at different % microwave powers (a) 10% (b) 20% (c) 30% (d) 40% at a scan rate of 50 mV/s.

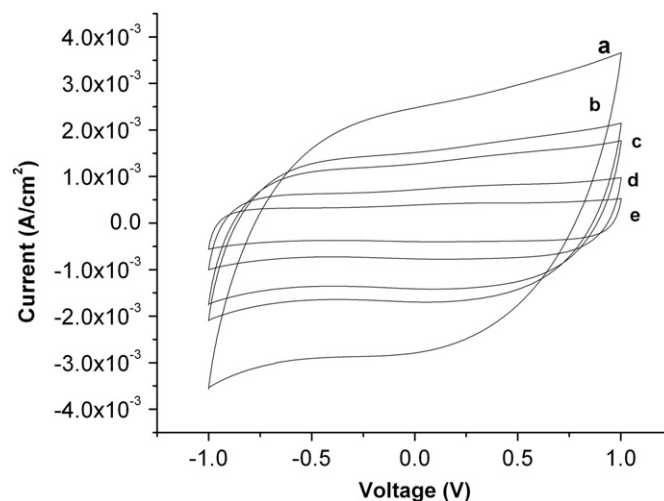


Fig. 7. CV for ZnO-AC (1:1) composite at scan rates, (a) 50 mV/s, (b) 25 mV/s, (c) 20 mV/s, (d) 10 mV/s, (e) 5 mV/s in 0.1 M Na₂SO₄.

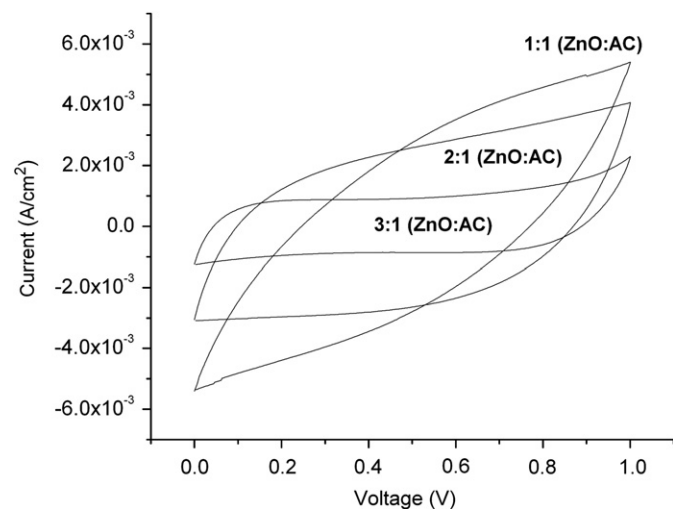


Fig. 5. CV for ZnO-AC composites at compositions of 1:1, 2:1 and 3:1.

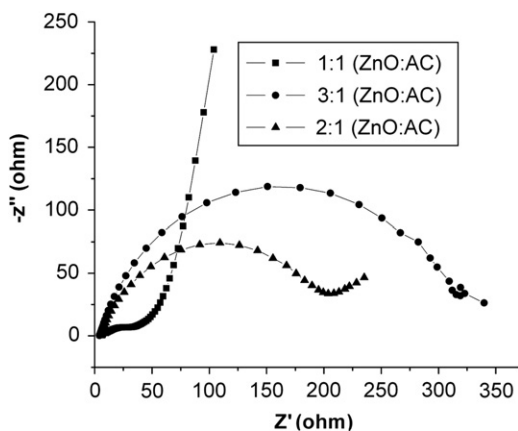


Fig. 6. Nyquist's plots for ZnO-AC composites at compositions of 1:1, 2:1 and 3:1.

The specific capacitance values of the various electrodes have been calculated from the respective cyclic voltammograms using the equation, $C = i/s$ where s is the potential sweep rate and i the

Table 1

Specific capacitance values of AC-ZnO electrodes and supercapacitor.

Materials	Scan rate (mV/s)	Specific capacitance (F/g)
AC-ZnO (1:1)	50	76
AC-ZnO (1:2)	50	55
AC-ZnO (1:3)	50	42
AC-ZnO (1:1)	50	76
	20	84
	10	105
	5	123
	2	160
Symmetrical supercapacitor	50	35
	20	47
	10	59
	5	75
	2	93

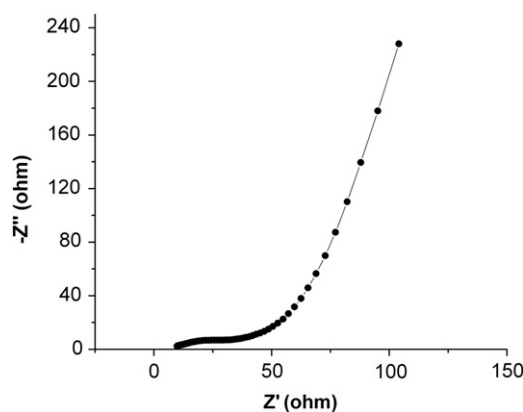


Fig. 8. Nyquist plot for the supercapacitor.

average current. The specific capacitance values of the electrodes and the supercapacitor have been tabulated in Table 1.

The AC impedance response (Nyquist plot) of p/p supercapacitor is shown in Fig. 8. A semicircle is obtained at high frequency in the range 100 KHz–10 Hz and a straight line in the low-frequency region. The capacitance value increases at low frequencies due to a larger number of ions moving which cause a

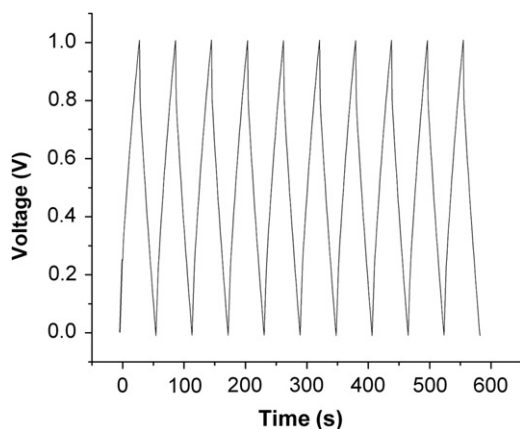


Fig. 9. Charge-discharge profile for the supercapacitor.

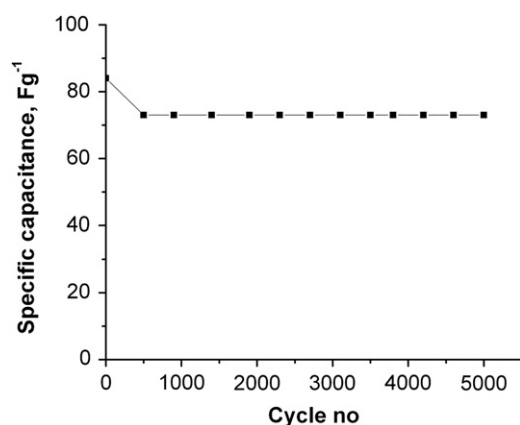


Fig. 10. Variation of specific capacitance of the supercapacitor under cyclings.

decrease in the bulk resistance of the capacitor. The semicircle results from the parallel combination of resistance and capacitance and the linear region is due to Warburg impedance. In the low frequency region, the linear region leans more towards imaginary axis and this indicates good capacitive behavior [14–16]. Hybrid capacitor and carbon capacitor electrodes behave

almost similarly in the high frequency region but AC–ZnO hybrid is more capacitive compared to simple carbon capacitors as is evident in the low frequency region. Fig. 9 shows the charge-discharge profile of the supercapacitor as measured by galvanostatic method at a current density of 6 mA cm^{-2} . The specific capacitance calculated under cyclings are, 84, 73 and 73 Fg^{-1} for 1st, 500th and 5000th cycle, indicating almost negligible decrease in the capacitance under cyclings (Fig. 10). This suggests that the supercapacitor is quite stable under cyclings.

4. Conclusions

In summary, nanostructured ZnO has been prepared by a facile microwave method and has been used to prepare electrodes by compositing with activated carbon. A p/p symmetrical hybrid supercapacitor has been fabricated using this composite electrodes and studied for their electrochemical properties by cyclic voltammetry, ac impedance spectroscopy and galvanostatic methods. The studies reveal that the supercapacitor has good capacitance and stable under cyclings. Hence ZnO–AC composites can be used effectively as supercapacitive active materials.

References

- [1] B.E. Conway, *Electrochemical Supercapacitors, Scientific Fundamentals and Technological applications*, Kluwer Academic Publishers, Plenum Press, New York, 1999.
- [2] I. Tanabashi, *J. Appl. Electrochem.* 35 (2005) 1067.
- [3] C.C. Hu, W.C. Chen, *Electrochem. Acta* 49 (2000) 3469.
- [4] J.P. Zheng, P.J. Cygann, T.R. Zon, *J. Electrochem. Soc.* 142 (1975) 2699.
- [5] K.C. Liu, M.A. Anderson, *J. Electrochem. Soc.* 143 (1996) 124.
- [6] V. Srinivasan, J.W. Weidner, *J. Electrochem. Soc.* 144 (1997) L210.
- [7] C. Lin, J.A. Ritter, B.N. Proper, *J. Electrochem. Soc.* 145 (1998) 4097.
- [8] S.C. Pang, M.A. Anderson, T.W. Chapman, *J. Electrochem. Soc.* 147 (2000) 444.
- [9] D.W. Chae, B.C. Kim, *J. Appl. Polym. Sci.* 99 (2006) 1854.
- [10] K. Nomura, H. Ohta, K. Weda, T. Kamiya, M. Hirano, H. Hosono, *Science* 300 (2003) 1269.
- [11] T. Yoshida, D. Komatsu, N. Shimokawa, H. Minoura, *Thin Solid Films* 451–452 (2004) 1269.
- [12] D. Kalpana, K.S. Omkumar, S. Suresh Kumar, N.G. Renganathan, *Electrochim. Acta* 52 (2006) 1309.
- [13] Denthaje Krishna Bhat, *Nanoscale Res. Lett.* 3 (2008) 31.
- [14] P. L. Taberna, P. Simon, J.F. Fauvarque, *J. Electrochem. Soc.* 150 (2003) A292.
- [15] M. SelvaKumar, D. Krishna Bhat, *J. Appl. Polym. Sci.* 107 (2008) 2165.
- [16] M. SelvaKumar, D. Krishna Bhat, *Physica B* 404 (2009) 1143.